Vol. 72: 73–82, 2017
https://doi.org/10.3354/cr01451

CLIMATE RESEARCH
Clim Res

Published online April 19

Drought assessment in northwest China during 1960–2013 using the standardized precipitation index

Peng Yang[1,2], Jun Xia[1,3,*], Yongyong Zhang[1], Longfeng Wang[1,2]

[1]Key Laboratory of Water Cycle & Related Land Surface Processes, Institute of Geographic Sciences and Natural Resources Research, Chinese Academy of Sciences, Beijing 100101, PR China
[2]University of Chinese Academy of Sciences, Beijing 100049, PR China
[3]State Key Laboratory of Water Resources & Hydropower Engineering Sciences, Wuhan University, Wuhan 430000, PR China

ABSTRACT: The standardized precipitation index (SPI) can be used to analyze the spatiotemporal characteristics of regional water resources. Monthly precipitation data obtained from 96 weather stations in northwest China from 1960 to 2013 were used to calculate the SPI. Changes in the SPI were analyzed using the Mann-Kendall (MK) test and the Pettitt test. The results indicated that 50 stations had a significant increasing trend in the annual SPI series. Analysis of seasonal SPI trends revealed the prevalence of serious drought conditions in the spring, while most stations exhibited a wetting trend in the winter. Significant (at $\alpha = 0.05$ level) abrupt changes in the annual and seasonal SPI series occurred mostly in 1981–1985. Additionally, a significant abrupt change occurred in the year 1986 in 5 sub-basins (the Turpan-Hami Basin, Gurbantunggut Desert Basin, Northern Tianshan Mountains, Northern Kunlun Mountains, and the Tarim Desert Basin).

KEY WORDS: Standardized precipitation index · Pettitt test · Mann-Kendall · Northwest China

1. INTRODUCTION

Droughts are a serious type of environmental disaster that adversely affect societies and economies around the world (Huang et al. 2015). The characteristics of a drought vary from one climate regime to another, which makes such climatological hazards difficult to study (Wilhite 2000, AghaKouchak et al. 2015). Temperatures have increased by ~0.75°C in the past 100 yr, and studies have observed a 0.18°C increase per decade during the last 25 yr due to climate change (Grover 2013). As a result of this warming, the global hydrological cycle has been altered, and there is an increasing likelihood of extreme events such as droughts and floods (Allan & Soden 2008). The spatiotemporal variability of dry spells and wet spells within a river basin can affect the socioeconomic development in the region (She et al. 2016). She et al. (2016) investigated the dry spells and wet spells in the Huaihe River Basin of China by using the copula function. Additionally, She et al. (2014) evaluated the dry spell frequency by applying L-moments in the middle reach of the Yellow River Basin, China, and She et al. (2013) detected the spatiotemporal variation and statistical characteristics of extreme dry spells in the Yellow River Basin.

In the past, droughts have been detected and monitored using various indices (Mishra & Singh 2011). The standardized precipitation index (SPI) was first proposed by McKee et al. (1993) to investigate and monitor hydrological conditions, and it has been widely adopted because of the its flexibility, stability, and simplicity (Bazrafshan et al. 2014). Notable studies that employed the SPI are as follows. Li et al. (2015) assessed the regional drought risk and trends in China. Ganguli & Reddy (2014) evaluated the

*Corresponding author: xiaj@igsnrr.ac.cn

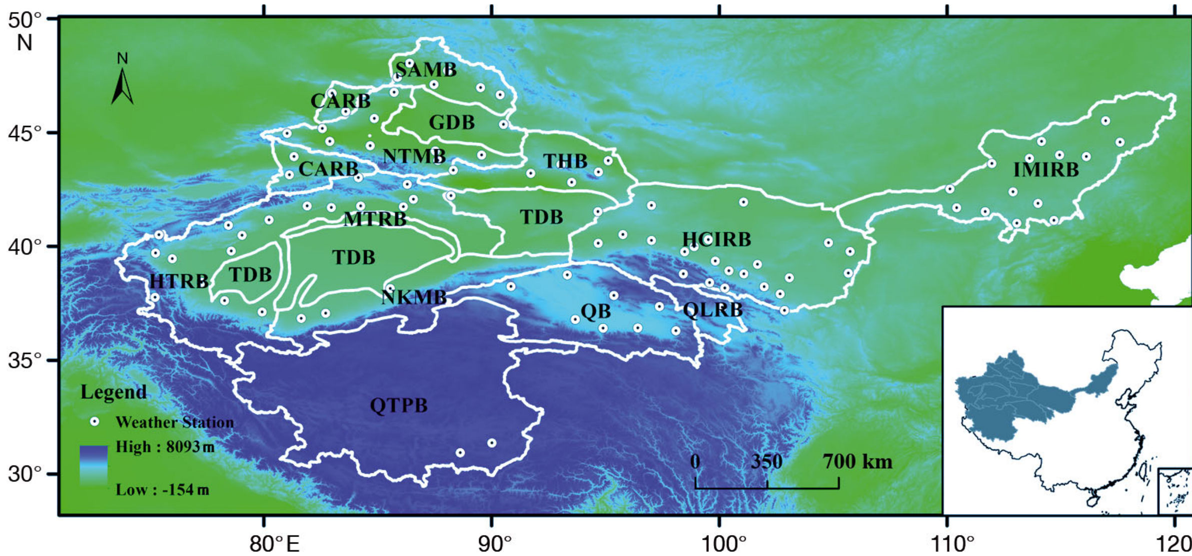

Fig. 1. The 14 sub-basins and 96 weather stations in northwest China considered in the calculation of the standard precipitation index (SPI) for the period 1960–2013. Code names of the sub-basins are defined in Table 1. Inset: Location of study area in China

trends and the multivariate frequency of droughts in 3 meteorological subdivisions of western India. Di Lena et al. (2014) analyzed the drought in the Abruzzo region of Central Italy. Ford & Labosier (2014) detected the spatial patterns of drought persistence in the southeastern United States, and He et al. (2015) investigated the spatiotemporal patterns of dry and wet conditions in the Huaihe River Basin.

Northwest China is susceptible to climate change because of its location in the middle of Eurasia, which experiences the effects of a complex atmospheric circulation system (He et al. 2015). Accurate assessments of changes in precipitation in northwest China are required to successfully manage the area's water resources. Assessments of the area have been conducted by several researchers. Notably, Chen et al. (2009) observed that precipitation in the Xinjiang Province has shown an increasing trend since the mid-1980s. Li et al. (2016) found that annual precipitation in the Xinjiang Province has increased by 26 mm since 1960, with a rate of increase of 4.12 mm per decade throughout the period 1960–2010. Deng et al. (2014) and Wang et al. (2013) investigated the spatial variations of extreme events in northwest China, focusing on precipitation extremes in the northern part of the Xinjiang Province. The development and subsequent occurrence of droughts are slow, continuous, and complex processes. Since there are no apparent warning signs of an impending drought, monitoring, identification, evaluation, and research on the occurrence and development of droughts would benefit efforts toward disaster prevention and mitigation, and aid in the adoption of suitable disaster relief countermeasures. Investigating droughts in northwest China would be particularly helpful for understanding the impacts on the region's economy and ecology. Many researchers have analyzed the spatiotemporal changes of precipitation trends in northwest China (Wang et al. 2013, Deng et al. 2014, Li et al. 2016). However, identifying abrupt change points in northwest China through SPI calculations is still needed to fully understand drought development.

To supply agricultural, ecological, and water resource management organizations in the region with useful information, we focus on the following topics in this study: (1) the conditions of precipitation resources in northwest China during the period 1960–2013; (2) the trends in the annual and seasonal SPI values; (3) the wet and dry periods at annual and seasonal scales for each station; and (4) abrupt change points experienced by sub-basins and individual stations at annual and seasonal scales.

2. STUDY AREA

The study area includes Xinjiang, Gansu, and some parts of Inner Mongolia, Hebei, Qinghai, and Tibet in China, and it spans an area of 3 362 260 km^2 (73° to 120° E, 30° to 50° N) (Fig. 1). The study area has a typical continental climate, with low precipitation (below 250 mm) and a wide mean annual temperature range (−2 to 19°C) (Deng et al. 2014). Because of the cold and dry weather conditions prevalent in

Table 1. Names and code names of 14 sub-basins in northwest China considered in the calculation of the standard precipitation index (SPI) for the period 1960–2013. See Fig. 1 for location of the sub-basins

Basin name	Basin code
Inner Mongolia Inland River Basin	IMIRB
Hexi Corridor Inland River Basin	HCIRB
Qinghai Lake River Basin	QLRB
Qaidam Basin	QB
Turpan-Hami Basin	THB
Southern Altay Mountain Basin	SAMB
Central Asia River Basin	CARB
Gurbantunggut Desert Basin	GDB
Northern Tianshan Mountain Basin	NTMB
Headstreams of the Tarim River Basin	HTRB
Northern Kunlun Mountain Basin	NKMB
Main stem of the Tarim River Basin[a]	MTRB
Tarim Desert Basin	TDB
Qiang Tang Plateau Basin	QTPB

[a]Excluded from study

winter, precipitation occasionally occurs as snow and ice. The land surface heats up quickly during the summer, and this feature combined with the low precipitation results in widespread desertification (Wang et al. 2013, Deng et al. 2014). In northwest China, there are many endothecia (inland) drainage basins and deserts (i.e. the Badanjilin Desert, Tengger Desert, Taklimakan Desert, Tsaidam Basin, Kubuqi Desert, and Tarim Basin).

The study area was divided into 14 sub-basins based on the division of water resources as given by the Ministry of Water Resources of the People's Republic of China (Fig. 1, Table 1). The main stem of the Tarim River Basin (MTRB) was excluded from our study as there was no meteorological station in the trunk stream.

3. MATERIALS AND METHODS

3.1. Data sources

For our analysis, we chose daily weather data from 96 weather stations in northwest China for the period 1960–2013, and the data were collected by the National Climate Center, China Meteorological Administration (CMA). Data from the stations installed after 1960 and those with vacant values were removed. We obtained monthly meteorological data, seasonal meteorological data, and annual meteorological data from the daily meteorological data collected at the 96 stations. We also obtained the average regional precipitation by taking the average precipitation value for all the stations in each sub-basin.

3.2. Methods

3.2.1. Standardized precipitation index

Originally, the SPI was calculated by using a 2-parameter gamma distribution (McKee et al. 1993) and, of late, the gamma distribution has been used to fit the probability distribution of precipitation (Wu et al. 2007). The details of SPI computation can be found in McKee et al. (1993).

However, there are difficulties with SPI interpretation when the precipitation data include zero values, and inconsistent SPI values can be obtained as a result of the adoption of parametric calculations in the traditional SPI calculation (Wu et al. 2007, Farahmand & AghaKouchak 2015, Stagge et al. 2015, Vergni et al. 2016). Wu et al. (2007) analyzed the possible errors and misleading interpretations of SPI values obtained in arid locations for zero precipitation, which was useful for our study. We applied the non-parametric methods suggested by Farahmand & AghaKouchak (2015) to get the marginal probability of precipitation by using the empirical Gringorten plotting position, instead of using a probability density function:

$$p(x_i) = (i - 0.44)/(n + 0.12) \qquad (1)$$

where n is the number of data points, x is precipitation accumulation, i represents the rank position of non-zero precipitation data from the minimum value in the data series, and $p(x_i)$ represents the corresponding empirical probability. Hence, SPI can be obtained from the outcome of Eq. (1) as follows:

$$\text{SPI} = \phi^{-1}(p) \qquad (2)$$

where ϕ stands for the standard normal distribution function and p is a product of Eq. (1).

In this study, the calculation of SPI was implemented by the Standardized Drought Analysis Toolbox (SDAT) developed by Farahmand & Agha Kouchak (2015). Positive SPI values represent wet periods, while the negative values represent dry periods.

While the 12 mo SPI values (SPI-12) in December were adopted for the annual trend analysis, SPI values for spring (MAM), summer (JJA), autumn (SON), and winter (DJF) were obtained from the 3 mo SPI values (SPI-3) in May, August, November, and February, respectively (He et al. 2015). Following the methods of He et al. (2015), dry and wet conditions

Table 2. Categories of dryness and wetness based on the standard precipitation index (SPI) values

SPI range	Category
SPI ≥ 2	Extremely wet
1.5 ≤ SPI < 2	Severely wet
1 ≤ SPI < 1.5	Moderately wet
−1 < SPI < 1	Near normal
−1.5 < SPI ≤ −1	Moderately dry
−2 < SPI ≤ −1.5	Severely dry
SPI ≤ −2	Extremely dry

were categorized into different levels based on the SPI values, as presented in Table 2.

3.2.2. Removing autocorrelation

Any autocorrelation in the atmospheric data would impact the trend analysis when commonly used standard statistical methods were applied (Wilks 2011). Therefore, we tested and deleted the significant autocorrelation in the series before applying the Mann-Kendall (MK) test. The statistic R, which was used to detect if the series were autocorrelated significantly, was obtained with Eqs. (3) & (4), as proposed by Box et al. (2008):

$$R = (1/n-1)\sum_{t-1}^{n-1}(x_t - \overline{x_t})(x_{t+1} - \overline{x_t}) / (1/n)\sum_{t-1}^{n}(x_t - \overline{x_t})^2 \quad (3)$$

$$(-1-1.96\sqrt{n-2})/(n-1) \le R \le (-1+1.96\sqrt{n-2})/(n-1) \quad (4)$$

where R is the lag-1 autocorrelation coefficient of x_t, where t is the time point. If R falls within the confidence limit, computed with Eq. (4), the autocorrelation is non-significant at an $\alpha = 5\,\%$ significance level. Otherwise, the previous time series would be replaced by the series $x_2 - r_1x_1$, $x_3 - r_1x_2$, …, $x_n - r_1x_{n-1}$, where r is the autocorrelation coefficient at lag time 1 mo.

3.2.3. Pettitt test

A turning point in the development of the SPI was the nonparametric Pettitt test proposed by Pettitt (1979). Based on the rank and distribution free testing, the unknown significant abrupt change points can be detected by the Pettitt test (Zhang & Lu 2009). The x_1, x_2, …, x_t and x_{t+1}, x_{t+2}, …, x_T sequences come from the time series of observations T (x_1, x_2, …, x_T). The $U_{t,T}$ (Mann-Whitney U, where t is the time of change point) are obtained from the following equation:

$$U_{t,T} = \sum_{i=1}^{t}\sum_{j=t+1}^{T}\text{sign}(x_i - x_j) 1 \le t < T \quad (5)$$

The possible change point (K_t) is obtained from:

$$K_t = \max|U_{t,T}| \quad (6)$$

The significance probability p associated with K_t is:

$$\text{p = 2exp[(−6Kt2)/(T3 + T2)]} \quad (7)$$

If $p < \alpha, x_t$ is regarded as a significant turning point at the significance level α.

The nonparametric Pettitt test was applied to detect whether the annual, spring, summer, autumn, and winter SPI series from the 96 stations contained abrupt change points where a significant change occurred.

3.2.4. Mann-Kendall trend test

The MK test is a nonparametric statistical test that is often applied to estimate the trend in a time series. The statistic variable S of the MK test can be computed as follows (Hirsch & Slack 1984):

$$S_t = \sum_{c=1}^{n-1}\sum_{d=c+1}^{n}\text{sign}(X_d - X_c) \quad (8)$$

$$\text{sign}(X_d - X_c) = \begin{cases} +1, X_d > X_c \\ 0, X_d = X_c \\ -1, X_d < X_c \end{cases} \quad (9)$$

where X_c, X_d are specific data points and n is the size of the series. The statistic Z can be obtained from Eqs. (10) & (11):

$$\text{Var}(S_t) = [n(n-1)(2n+5) - \sum_{c=1}^{n} t_c(c)(c-1)(2c+5)]/18 \quad (10)$$

$$Z = \begin{cases} (S_t - 1)/\sqrt{\text{Var}(S_t)}, & S_t > 0 \\ 0, & S_t < 0 \\ (S_t + 1)/\sqrt{\text{Var}(S_t)}, & S_t = 0 \end{cases} \quad (11)$$

where t_c is the cumulative value for t and c represents the number of duplicates. We have chosen $\alpha = 0.05$ to be the significance level in this article, which means $|Z| > Z_{1-\alpha/2} = 1.96$.

The modified MK test was applied to investigate the trends in the annual and seasonal SPI for the 96 weather stations. Before using the MK trend test, we checked and removed the autocorrelation of each SPI series by applying the above methods. In the study area, 8, 11, 6, 4, and 19 stations had autocorrelations that reached significant levels during the annual, spring, summer, fall, and winter SPI series, respectively.

4. RESULTS AND DISCUSSION

4.1. Precipitation resource distribution

From 1960 to 2013, the annual average precipitation in northwest China was 179 mm with a standard deviation of 112 mm. The highest annual precipitation was 228 mm in 2010, which was 54.7% higher than the lowest amount of 147 mm in 1997. The 13 sub-basins in northwest China had varying precipitation levels. QLRB had the highest average annual precipitation (381 mm), followed by CARB (329 mm), QTPB (320 mm), IMIRB (260 mm), SAMB (182 mm), GDB (176 mm), NTMB (164 mm), HCIRB (156 mm), and HTRB (114 mm). The basins with lower precipitation rates were QB (82 mm), THB (80 mm), TDB (50 mm), and NKMB (38 mm) (see Table 1 for sub-basin codes and Fig.1 for their location in northwest China). Similarly, the highest variation in annual precipitation was exhibited in QTBP with a standard deviation of 65 mm, followed by CARB (62 mm). The 3 smallest variations of annual precipitation were in TDB (18 mm), THB (19 mm), and NKMB (21 mm) (as shown in Table 3).

Because of impacts from the regional continental climate, the 13 water sub-basins displayed seasonal precipitation distributions, with the highest levels in summer (JJA) and the lowest levels in winter (DJF). The seasonal proportions of annual precipitation varied greatly in the 13 sub-basins; specifically, spring precipitation accounted for between 7.9 and 27.7% of the annual precipitation, summer precipitation accounted for between 33.8 and 71.4%, fall precipitation accounted for between 8.9 and 27.2%, and winter precipitation accounted for between 1 and 16.7% (Table 3). The large flux in seasonal contributions to the annual precipitation illustrates its variability across the study region and highlights the importance of modeling at multiple scales.

4.2. Trend analysis of SPI series

For 1960–2013, annual SPI values showed downward trends at 12 stations, and upward trends at 84 stations. Fifty stations with increasing trends were located in QTPB, QLRB, HCIRB, HTRB, SAMB, QB, THB, NTMB, and CARB, and these trends were significant at a 90% confidence level. Only 1 station, which was located in THB, showed a decreasing trend at the 90% confidence level. Stations with increasing trends were located in every sub-basin of the study area, although 24 of them were non-significant. The stations with decreasing trends were located in HCIRB and IMIRB, but 11 of those stations showed non-significant trends. In addition, 69.2% of the stations located in IMIRB exhibited downward trends in the annual SPI without reaching a 90% confidence level (Fig. 2). The annual trends revealed significant differences among the sub-basins examined. The larger regional trend suggests that the SPI is increasing, while the risk of drought is increasing in IMIRB.

The seasonal SPI values had significantly different modes. A wetting trend could be observed in the 4 seasons; in spring, 79 stations exhibited an upward trend in SPI-3 and 17 stations exhibited a downward trend. Though some trends were non-significant, the

Table 3. Annual and seasonal precipitation in the 13 sub-basins of the study area in northwest China during 1960–2013. Seasonal data shows totals (mm) and the proportion of annual precipitation (%) that occurred in the season concerned. See Table 1 for definition of sub-basin code names and Fig. 1 for their locations

Site	Annual	Spring		Summer		Fall		Winter	
	(mm)	(mm)	(%)	(mm)	(%)	(mm)	(%)	(mm)	(%)
IMIRB	260	35	13.6	174	66.8	45	17.2	6	2.4
HCIRB	157	26	16.8	96	61.5	30	19.4	4	2.4
QLRB	381	57	14.9	249	65.4	71	18.7	4	1.0
QB	82	16	19.4	51	62.7	11	13.1	4	4.8
THB	80	14	17.1	48	59.6	14	18.1	4	5.2
SAMB	182	41	22.3	62	33.8	49	27.2	30	16.7
CARB	329	91	27.7	126	38.4	71	21.5	41	12.5
GDB	176	38	21.7	86	48.6	37	21.2	15	8.4
NTMB	164	46	27.9	67	40.5	34	20.6	18	10.9
HTRB	114	27	23.3	62	54.8	18	16.0	7	5.9
NKMB	38	10	24.8	23	59.3	3	9.1	3	7.0
TDB	50	9	16.2	33	65.8	7	13.4	2	4.4
QTPB	320	25	7.9	228	71.4	63	19.5	4	1.2

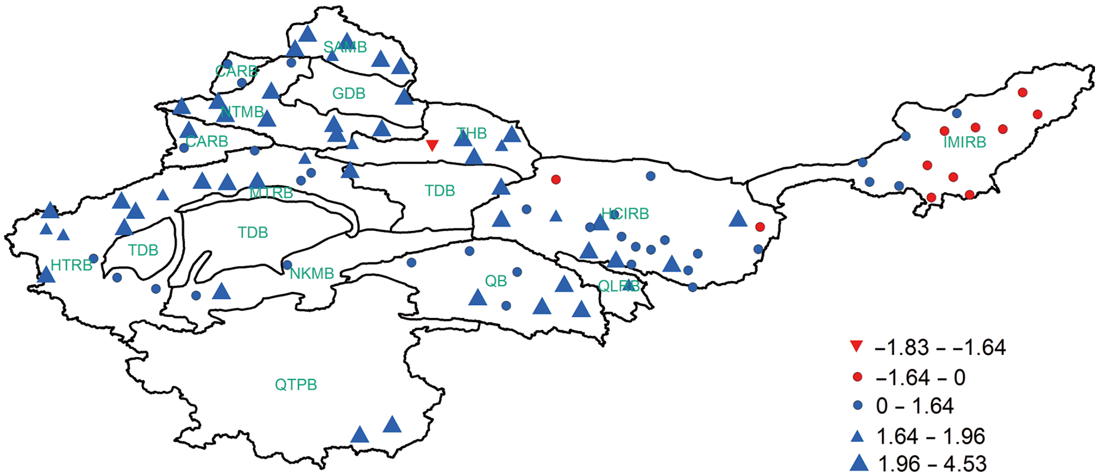

Fig. 2. Annual SPI trends at the 96 weather stations in northwest China between 1960 and 2013. Upward-pointing (blue) and downward-pointing (red) triangles represent wetting and drying trends, respectively. The size of the triangles indicates significant trends at different confidence levels. Sub-basin code names defined in Table 1

results suggest that seasonal changes occurred over 1960–2013. All the stations in IMIRB, QB, QTPB, NTMB, SAMB, and GDB displayed a wetting tendency in the spring. Conversely, some stations in HCIRB, QLRB, THB, CARB, HTRB, NKMB, and MTRB exhibited drying trends in the spring. Most of these stations were clustered in the western part of the study area; therefore, it is possible that Xinjiang Province could experience droughts of greater severity in the spring. Another season with a drying trend was fall, with 21 stations exhibiting decreasing trends during this time, although the trends were not significant. Twelve stations showed a significant wetting trend in the fall at the 95% confidence level. These stations were located in IMIRB, HCIRB, THB, NTMB, and HTRB. Seven stations exhibited a wetting trend with a 90% confidence level (Fig. 3). Changes in the seasonal dryness or wetness patterns could contribute to decreased agricultural yields and potential flooding, respectively.

In summer, 76 stations showed an upward trend in SPI-3 with 12 stations showing significant changes at the 90% confidence level. All the stations in the QTPB, QLRB, THB, GDB, and QB sub-basins showed an upward trend in seasonal SPI. By contrast, 13 of the 14 stations in IMIRB demonstrated a drying trend in the summer, including 2 stations with results that were significant at the 90% confidence level; the results for the other 11 stations were not significant. In winter, the stations that showed significant increasing trends were clustered in the western part of northwest China, in CARB, GDB, NKMB, THB, and QB (Fig. 3d). Two stations in the IMIRB and 3 stations in the HCIRB showed non-significant decreasing trends in the winter.

Many researchers have focused on the spatiotemporal properties of precipitation at the annual and different seasonal scales in northwest China. Li et al. (2015) applied statistical methods to analyze precipitation features, and they found that precipitation showed a significant upward trend at the rate of 0.61 mm yr^{-1} ($p < 0.01$) in northwest China; this was probably due to changes in the western Pacific subtropical high (WPSH) and the North Atlantic subtropical high (NASH). Huang et al. (2015) used 2 indices (the precipitation concentration index and the concentration index) to investigate diversiform precipitation in the Qinghai Province. The results showed that while the monthly precipitation distribution showed significant irregularity, the daily precipitation showed a highly homogeneous distribution of precipitation concentration. Deng et al. (2014) found that the values of the tested precipitation extreme indices had strong regional variations, and the increasing trend in northern Xinjiang was stronger than that in the southern Xinjiang and the Hexi Corridor. The increasing trends were not remarkable in the Hexi Corridor, with 3 out of the 4 tested indices being statistically non-significant at the 0.05 level in 1960–2010. Zhang et al. (2015) found that the precipitation series had increasing trends in JJA and DJF. A decreasing trend in precipitation was found in 33% of stations in the spring series, and 11% had a decreasing trend in the fall. At the same time, the SPI-12 values of all the stations had an increasing trend in the Aksu River Basin in 1960–2010.

4.3. Abrupt changes in annual and seasonal SPI series

The abrupt change points of annual precipitation in the 13 sub-basins in northwest China at a 95% confidence level are shown in Table 4. The abrupt change point for 5 of the sub-basins (i.e. THB, GDB, NTMB, NKMB, and TDB) was in the 1986; another 5 sub-basins exhibited no abrupt change point; 4 sub-basins had unique abrupt change points in the years 1992 (SAMB) and 1997 (CARB). The trends before and after the abrupt change points were very distinct.

For the SPI-12, there were 38 stations that showed an abrupt change point at a 95% confidence level in northwest China in 1960–2013 (Fig. 4). Two stations (from IMIRB and HCIRB) showed an abrupt change point in 1966–1970. One station from HCIRB showed an abrupt change point from 1960–1965. In 1971–1975, 4 stations (one from QB, one from HCIRB, and 2 from IMIRB) showed abrupt change points. Abrupt change points were observed at 2 stations in 1976–1980. While 15.6% of the stations exhibited an abrupt change point in 1981–1985, 9.3% of the stations, most of them from the Xinjiang Province, displayed abrupt change points in 1986–1990. While 3 stations exhibited abrupt change points in 1991–1995, 2 stations exhibited abrupt change points in 1996–2000. These results prove that the precipitation in the Xinjiang Province underwent a large change in 1981–1990. The number of stations with abrupt change points was comparable to those determined by Chen et al. (2014), who found that an abrupt change of precipitation extremes occurred in northwest China in 1986.

Seasonal abrupt change points at a 95% confidence level were detected at 52 stations, 47 stations, 29 stations, and 35 stations during spring, summer, fall, and winter, respectively (Fig. 5). The significant abrupt changes in the spring and summer SPI series were

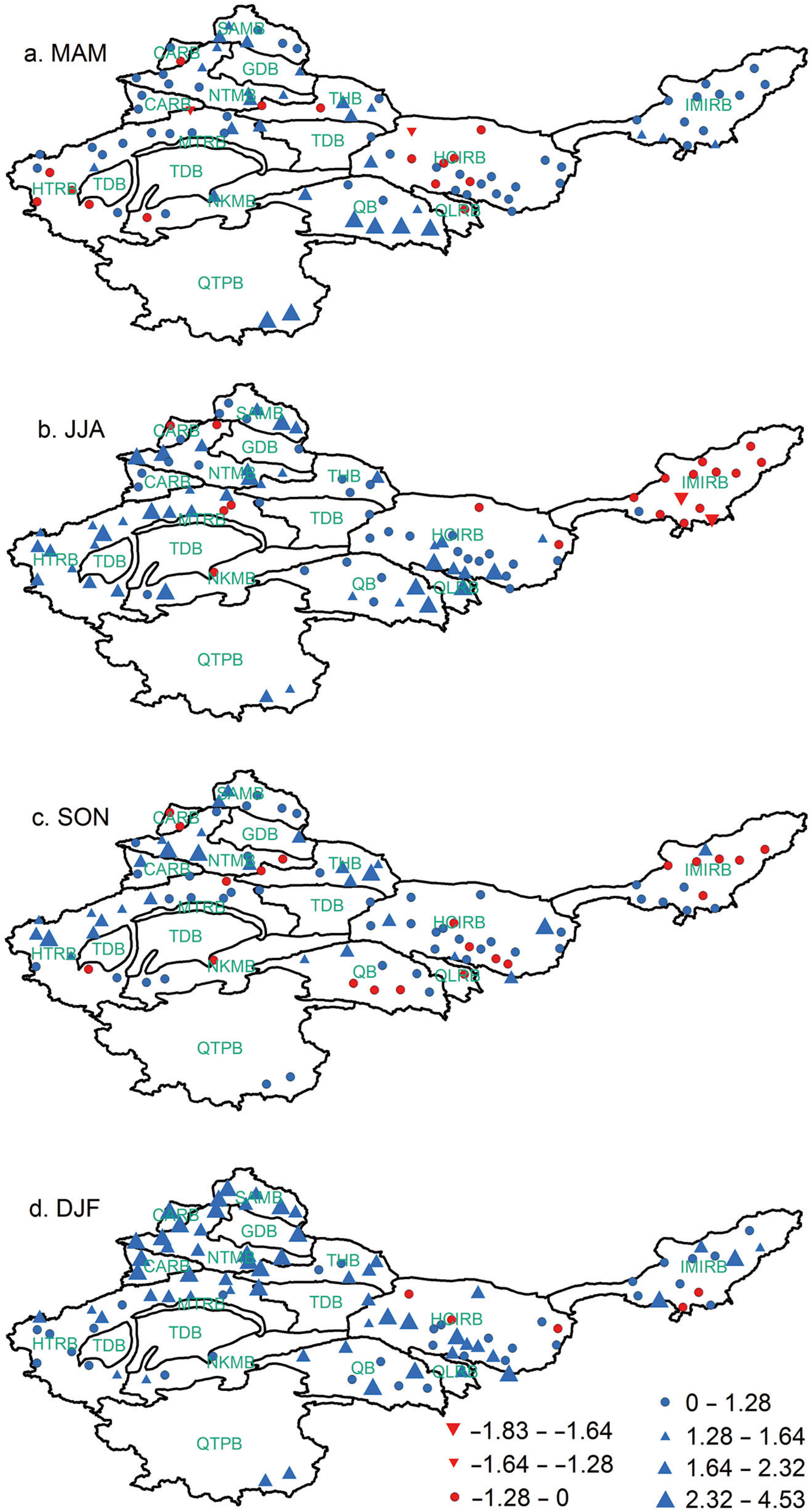

Fig. 3. Seasonal SPI trends at the 96 rain stations in the northwest China between 1960 and 2013. Upward-pointing (blue) and downward-pointing (red) arrows represent wetting and drying trends, respectively. Size of the triangles indicates significant trends at different confidence levels (see Fig. 2 legend for further explanation)

similar to each other in northwest China. The significant abrupt change points at 17 stations were between 1981 and 1985 in spring and summer. In addition, there were 10 stations in Northwest China with abrupt change points in the fall SPI series ($p < 0.005$) from 1981 to 1985, and 20 stations had abrupt change points in the winter SPI series at a 95% confidence level between 1981 and 1985. Thus, the significant abrupt change points were mostly in the early and mid-1980s. The period with the second highest number of stations showing significant abrupt change points were 1971–1975 in spring (12 stations) and summer, 1976–1980 in autumn and 1971–1975 and 1986–1990 in winter. Based on seasonal data, the range of abrupt change over the study period was found to be from 1970 to 1990.

5. CONCLUSION

The annual and seasonal SPI series in northwest China were obtained from the rainfall data from 96 stations for 1960–2013. Study results showed that northwest China underwent severe wet and dry conditions at every station at least once during the study period. Most of the stations had increasing annual trends in SPI; however, many trends were non-significant (Fig. 3). For most stations, the wetting trend prevailed in the winter. Drying trends in the spring were significant at 2 stations in northwest China (in HCIRB and HTRB) (Fig. 4a). Similarly, drying trends in summer and fall were significant at 2 stations located in HCIRB. The significant abrupt change points of the annual and all seasonal SPI series occurred mostly in the period 1981–1985.

Table 4. Pettitt test results for annual precipitation in 13 subbasins in northwest China during 1960–2013, showing time points when abrupt changes in precipitation trends occurred and, in each case, precipitation trends before and after the change occurred. See Table 1 definition of subbasin to code names. –: no abrupt change

Code name	Abrupt change time points	Change trend (mm yr^{-1}) Pre-change	Post-change
IMIRB	–	–	–
HCIRB	–	–	–
QLRB	–	–	–
QB	–	–	–
THB	1986	0.22	–0.29
SAMB	1992	0.98	0.68
CARB	1997	–0.3	–2.92
GDB	1986	–0.23	–2.3
NTMB	1986	0.17	0.33
HTRB	–	–	–
NKMB	1986	–0.19	0.18
TDB	1986	0.26	–0.24
QTPB	–	–	–

The annual and seasonal SPI series exhibited various conditions in northwest China. Changing SPIs represent shifts in precipitation, which could influence the region's hydrological regime and in turn affect crop yields, habitat diversity, and water resource management in the region (He et al. 2015). The long-term analysis results of this study indicate that if the current trends in SPI continue, we can expect spring droughts of greater severity in northwest China. Assuming that the trends evident in this study are due to climate change, the hydrology of northwest China will continue to be altered unless mitigation measures are implemented. If winter precipitation continues to increase as suggested by the

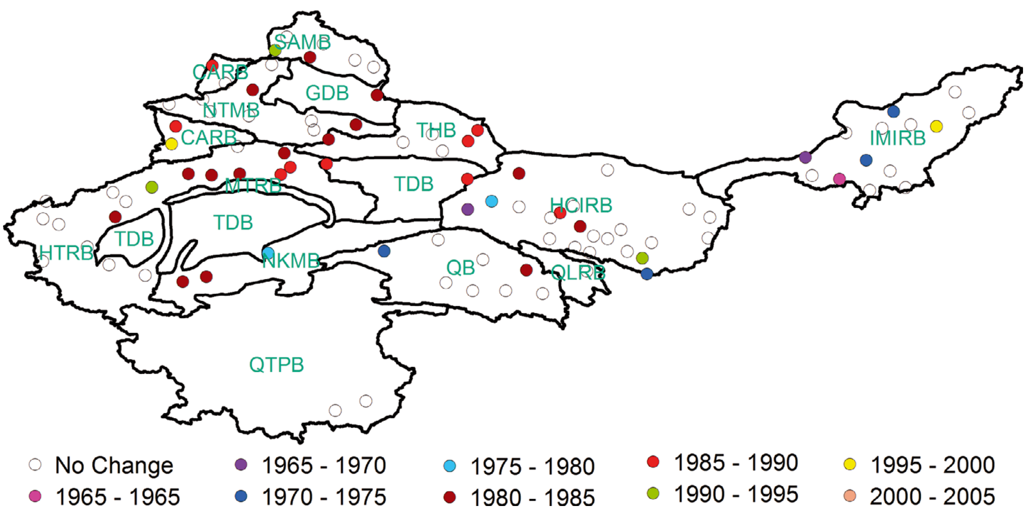

Fig. 4. Distribution of the years with abrupt changes in the annual SPI series at weather stations in northwest China. Subbasin code names defined in Table 1

winter SPI series, storm events that include ice and snow hazards will likely occur, along with water resource management issues, as a result of the increased occurrences of spring melt events.

There is a need to identify the drivers of change in precipitation and develop feasible adaptation strategies for utilizing water resources sustainably in northwest China. Possible drivers of precipitation in the region include the geomorphic and topographic characteristics that directly impact the spatial patterns of dryness/wetness conditions in Qinghai (Liu et al. 2013). Another potential factor is atmospheric circulation, which could affect the water vapor transformation and the hydrological cycle. For example, the Indian summer monsoon primarily effects the precipitation in the Tuotuo River (Liu et al. 2013); the western circulation at mid-latitudes plays a principal role in the precipitation in the Qaidam Basin in the spring and winter (Qian & Qin 2008); the East Asian summer monsoon is associated with dryness/wetness conditions in the Qilian Mountains (Wang 2001); WPSH and NASH might have been chiefly responsible for the significant increase in the rainfall of northwest China for 1980–2010 (Li et al. 2016). In addition, El Niño events on multi-year scales could be linked to variances in the precipitation in northwest China (Liu et al. 2016). The differences in the different periodic components and their composite effects on the trends of the original precipitation series may have been due to the aforementioned phenomena. However, these are just probable causes, not definite explanations. Full comprehension of precipitation variability and an improved ability to forecast rainfall at temporal and spatial scales would benefit from a thorough understanding of the relationships between the precipitation and the factors affecting it in this region.

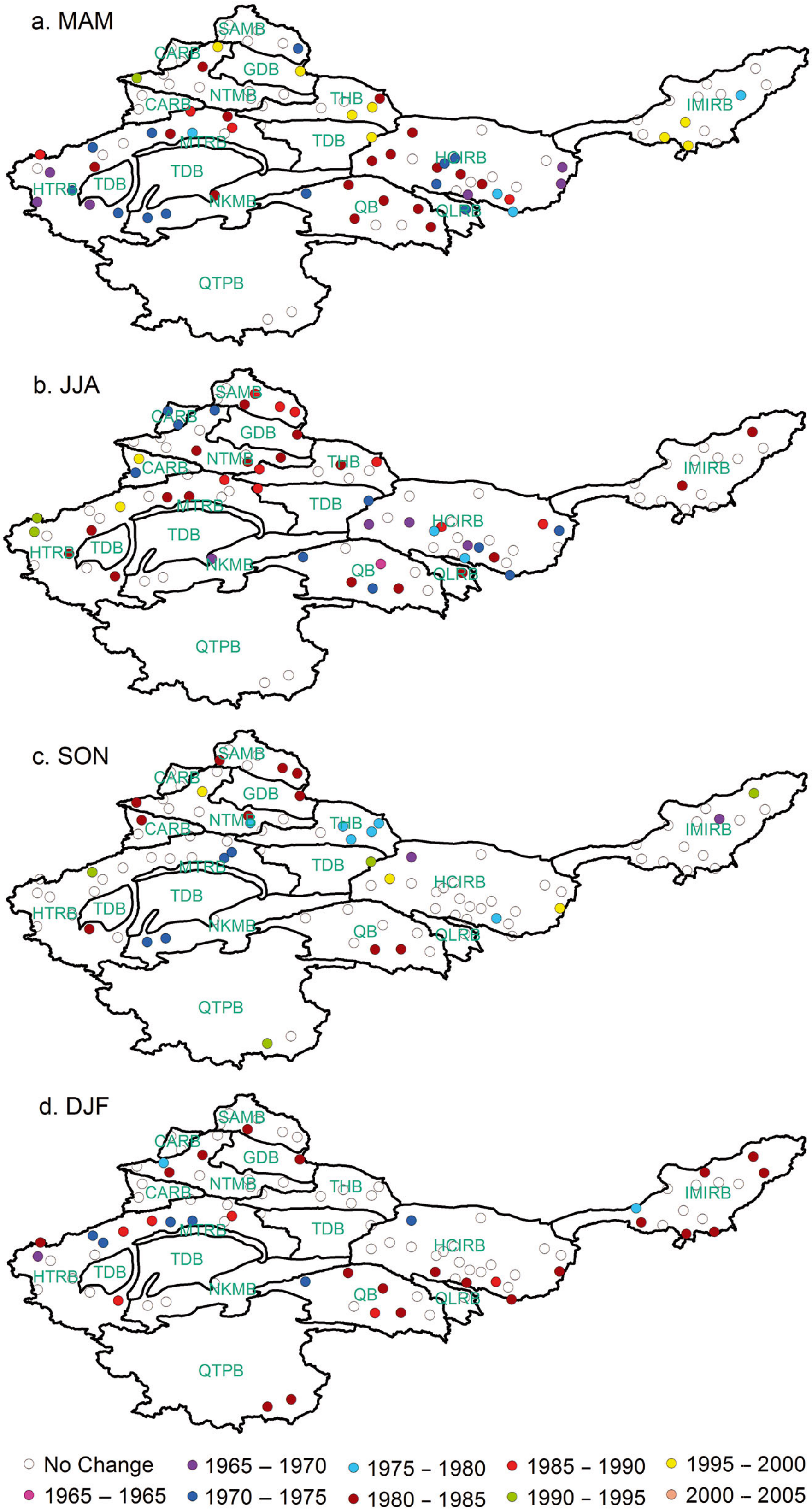

Fig. 5. Distribution of the years with abrupt changes in the seasonal SPI series at weather stationsin northwest China. Sub-basin code names defined in Table 1

Acknowledgements. The research was supported by the National Basic Research Program of China (973 Program: 2012CB956204). The authors thank the National Climate Center, China Meteorological Administration, for providing the meteorological data for this study. The authors also thank the reviewers for making beneficial suggestions.

LITERATURE CITED

AghaKouchak A, Farahmand A, Melton FS, Teixeira J, Anderson MC, Wardlow BD, Hain CR (2015) Remote sensing of drought: progress, challenges and opportunities. Rev Geophys 53:452–480

Allan RP, Soden BJ (2008) Atmospheric warming and the amplification of precipitation extremes. Science 321: 1481–1484

Bazrafshan J, Hejabi S, Rahimi J (2014) Drought monitoring using the multivariate standardized precipitation index (MSPI). Water Resour Manage 28:1045–1060

Box GEP, Jenkins GM, Reinsel GC (2008) Time series analysis, forecasting and control, 4th edn. John Wiley & Sons, New York, NY

Chen YN, Xu CC, Yang YH, Hao XM and others (2009) Hydrology and water resources variation and its responses to regional climate change in Xinjiang. Acta Geogr Sin 64:1331–1341 (in Chinese)

Chen YN, Deng HJ, Li BF, Xu CC (2014) Abrupt change of temperature and precipitation extremes in the arid region of Northwest China. Quat Int 336:35–43

Deng HJ, Chen YN, Shi X, Li WH, Wang H, Zhang S, Fang G (2014) Dynamics of temperature and precipitation extremes and their spatial variation in the arid region of northwest China. Atmos Res 138:346–355

Di Lena B, Vergni L, Antenucci F, Todisco F, Mannocchi F (2014) Analysis of drought in the region of Abruzzo (Central Italy) by the Standardized Precipitation Index. Theor Appl Climatol 115:41–52

Farahmand A, AghaKouchak A (2015) A generalized framework for deriving nonparametric standardized drought indicators. Adv Water Resour 76:140–145

Ford T, Labosier CF (2014) Spatial patterns of drought persistence in the Southeastern United States. Int J Climatol 34:2229–2240

Ganguli P, Reddy MJ (2014) Evaluation of trends and multivariate frequency analysis of droughts in three meteorological subdivisions of western India. Int J Climatol 34: 911–928

Grover VI (2013) Impact of climate change on water and health. CRC Press, Boca Raton, FL

He Y, Ye JY, Yang XY (2015) Analysis of the spatio-temporal patterns of dry and wet conditions in the Huai River Basin using the standardized precipitation index. Atmos Res 166:120–128

Hirsch RM, Slack JR (1984) A nonparametric trend test for seasonal data with serial dependence. Water Resour Res 20:727–732

Huang SZ, Huang Q, Chang JX, Zhu YL Leng G, Xing L (2015) Drought structure based on a nonparametric multivariate standardized drought index across the Yellow River basin, China. J Hydrol 530:127–136

Li XZ, Zhou W, Chen Y, David Q (2015) Assessment of regional drought trend and risk over China: a drought climate division perspective. J Clim 28:7025–7037

Li BF, Chen YN, Chen ZS, Xiong HG, Lian L (2016) Why does precipitation in northwest China show a significant increasing trend from 1960 to 2010? Atmos Res 167: 275–284

Liu Z, Zhou P, Zhang F, Liu X, Chen G (2013) Spatiotemporal characteristics of dryness/wetness conditions across Qinghai Province, Northwest China. Agric For Meteorol 182-183:101–108

Liu Z, Menzel L, Dong C, Fang R (2016) Temporal dynamics and spatial patterns of drought and the relation to ENSO: a case study in Northwest China. Int J Climatol 36: 2886–2898

McKee TB, Doesken NJ, Kleist J (1993) The relationship of drought frequency and duration to time scales. Preprints Eighth Conference on Applied Climatology, 17–22 Jan 1993, Anaheim, CA. American Meteorolical Society, Boston, MA, p 179–184

Mishra AK, Singh VP (2011) Drought modeling — a review. J Hydrol 403:157–175

Pettitt AN (1979) A non-parametric approach to the change-point problem. J R Stat Soc C 28:126–135

Qian WH, Qin AM (2008) Precipitation division and climate shift in China from1960 to 2000. Theor Appl Climatol 93: 1–17

She DX, Xia J, Song JY, Du H, Chen J, Wan L (2013) Spatio-temporal variation and statistical characteristic of extreme dry spell in Yellow River Basin, China. Theor Appl Climatol 112:201–213

She DX, Xia J, Zhang D, Ye AZ, Sood A (2014) Regional extreme-dry-spell frequency analysis using L-moments method in the middle reach of Yellow River Basin, China. Hydrol Processes 28:4694–4707

She DX, Mishra AK, Xia J, Zhang LP, Zhang X (2016) Wet and dry spell analysis using copulas. Int J Climatol 36: 476–491

Stagge JH, Tallaksen LM, Gudmundsson L, Van Loon AF, Stahl K (2015) Candidate distributions for climatological drought indices (SPI and SPEI). Int J Climatol 35: 4027–4040

Vergni L, Todisco F, Mannocchi F (2016) Evaluating the uncertainty and reliability of standardized indices. Hydrol Res 48, http://hr.iwaponline.com/content/early/2016/08/30/nh.2016.076

Wang HJ (2001) The weakening of the Asian monsoon circulation after the end of 1970's. Adv Atmos Sci 18: 376–386

Wang HJ, Chen YN, Chen ZS (2013) Spatial distribution and temporal trends of mean precipitation and extremes in the arid region, northwest of China, during 1960–2010. Hydrol Processes 27:1807–1818

Wilhite DA (2000) Drought as a natural hazard: concepts and definitions. In: Wilhite DA (ed) Drought: a global assessment. Routledge, London, p 3–18.

Wilks DS (2011) Statistical methods in the atmospheric sciences, 3rd edn. Academic Press, Cambridge, MA

Wu H, Svoboda MD, Hayes MJ, Wilhite A, Wen F (2007) Appropriate application of the standardized precipitation index in arid locations and dry seasons. Int J Climatol 27:65–79

Zhang S, Lu XX (2009) Hydrological responses to precipitation variation and diverse human activities in a mountainous tributary of the lower Xijiang, China. Catena 77: 130–142

Zhang YH, Cai WY, Chen QH, Yao YJ, Liu K (2015) Analysis of changes in precipitation and drought in Aksu River Basin, northwest China. Adv Meteorol 2015:215840

Editorial responsibility: Eduardo Zorita, Geesthacht, Germany

Submitted: July 11, 2016; Accepted: December 9, 2016
Proofs received from author(s): March 15, 2017